REPORT DOCUMENTATION PAGE

Form Approved OMB NO. 0704-0188

1. REPORT DATE (DD-MM-YYYY)	2. REPORT TYPE	3. DATES COVERED (From - To)
	New Reprint	-

4. TITLE AND SUBTITLE	5a. CONTRACT NUMBER
Design and optimization of a light-emitting diode projection micro-stereolithography three-dimensional manufacturing system	
	5b. GRANT NUMBER
	W911NF-07-D-0004
	5c. PROGRAM ELEMENT NUMBER
	611104

6. AUTHORS	5d. PROJECT NUMBER
Christopher M. Spadaccini, Xiaoyu Zheng, Joshua Deotte, Matthew P. Alonso, George R. Farquar, Todd H. Weisgraber, Steven Gemberling, Howon Lee, Nicholas Fang	
	5e. TASK NUMBER
	5f. WORK UNIT NUMBER

7. PERFORMING ORGANIZATION NAMES AND ADDRESSES	8. PERFORMING ORGANIZATION REPORT NUMBER
Massachusetts Institute of Technology (MIT) Office of Sponsored Programs 77 Massachusetts Avenue Cambridge, MA 02139 -4307	

9. SPONSORING/MONITORING AGENCY NAME(S) AND ADDRESS(ES)	10. SPONSOR/MONITOR'S ACRONYM(S)
U.S. Army Research Office P.O. Box 12211 Research Triangle Park, NC 27709-2211	ARO
	11. SPONSOR/MONITOR'S REPORT NUMBER(S)
	52900-CH-ISN.320

12. DISTRIBUTION AVAILIBILITY STATEMENT

Approved for public release; distribution is unlimited.

13. SUPPLEMENTARY NOTES

The views, opinions and/or findings contained in this report are those of the author(s) and should not contrued as an official Department of the Army position, policy or decision, unless so designated by other documentation.

14. ABSTRACT

The rapid manufacture of complex three-dimensional micro-scale components has eluded researchers for decades. Several additive manufacturing options have been limited by either speed or the ability to fabricate true three-dimensional structures. Projection micro-stereolithography (P?SL) is a low cost, high throughput additive fabrication technique capable of generating three-dimensional microstruc- tures in a bottom-up, layer by layer fashion. The P?SL system is reliable and capable of manufactur- ing a variety of highly complex, three-dimensional

15. SUBJECT TERMS

light emitting diodes, manufacturing processes, masks, optimisation, polymerisation, stereolithography

16. SECURITY CLASSIFICATION OF:			17. LIMITATION OF ABSTRACT	15. NUMBER OF PAGES	19a. NAME OF RESPONSIBLE PERSON
a. REPORT	b. ABSTRACT	c. THIS PAGE	UU		John Joannopoulos
UU	UU	UU			19b. TELEPHONE NUMBER
					617-253-4806

Design and optimization of a light-emitting diode projection micro-stereolithography three-dimensional manufacturing system

ABSTRACT

The rapid manufacture of complex three-dimensional micro-scale components has eluded researchers for decades. Several additive manufacturing options have been limited by either speed or the ability to fabricate true three-dimensional structures. Projection micro-stereolithography (P?SL) is a low cost, high throughput additive fabrication technique capable of generating three-dimensional microstruc- tures in a bottom-up, layer by layer fashion. The P?SL system is reliable and capable of manufactur- ing a variety of highly complex, three-dimensional structures from micro- to meso-scales with micro- scale architecture and submicron precision. Our P?SL system utilizes a reconfigurable digital mask and a 395 nm light-emitting diode (LED) array to polymerize a liquid monomer in a layer-by-layer manufacturing process. This paper discusses the critical process parameters that influence polymer- ization depth and structure quality. Experimental characterization and performance of the LED-based P?SL system for fabricating highly complex three-dimensional structures for a large range of appli- cations is presented.

Continuation for Block 13

ARO Report Number   52900.320-CH-ISN
Design and optimization of a light-emitting diode   ...

Block 13: Supplementary Note

Design and optimization of a light-emitting diode projection micro-stereolithography three-dimensional manufacturing system

Xiaoyu Zheng,[1] Joshua Deotte,[1] Matthew P. Alonso,[1,2] George R. Farquar,[1] Todd H. Weisgraber,[1] Steven Gemberling,[1] Howon Lee,[3] Nicholas Fang,[3] and Christopher M. Spadaccini[1]

[1]*Lawrence Livermore National Laboratory, Livermore, California 94550, USA*
[2]*Department of Mechanical Science and Engineering, University of Illinois at Urbana Champaign, Illinois 61801, USA*
[3]*Department of Mechanical Engineering, Massachusetts Institute of Technology, Cambridge, Massachusetts 02139, USA*

The rapid manufacture of complex three-dimensional micro-scale components has eluded researchers for decades. Several additive manufacturing options have been limited by either speed or the ability to fabricate true three-dimensional structures. Projection micro-stereolithography (PμSL) is a low cost, high throughput additive fabrication technique capable of generating three-dimensional microstructures in a bottom-up, layer by layer fashion. The PμSL system is reliable and capable of manufacturing a variety of highly complex, three-dimensional structures from micro- to meso-scales with micro-scale architecture and submicron precision. Our PμSL system utilizes a reconfigurable digital mask and a 395 nm light-emitting diode (LED) array to polymerize a liquid monomer in a layer-by-layer manufacturing process. This paper discusses the critical process parameters that influence polymerization depth and structure quality. Experimental characterization and performance of the LED-based PμSL system for fabricating highly complex three-dimensional structures for a large range of applications is presented. © *2012 American Institute of Physics*. [http://dx.doi.org/10.1063/1.4769050]

I. INTRODUCTION

The ability to produce complex, micro-scale, three-dimensional (3D) structures is a major challenge for the manufacturing industry. These types of structures can provide highly functional components for a variety of applications such as bioimplantable devices, sensors and actuators, micro-robots, thermal electronics, and energy efficient structures.[1–5]

There is a large array of additive methods to fabricate 3D structures. Current manufacturing of 3D microstructures involves highly complex processes such as x-ray lithography,[6] deep UV,[7] LIGA,[8] and soft lithography.[9] In all these manufacturing technologies, the fabrication of the final structures cannot be completed with a single process, and also requires large quantities of sacrificial material. These technologies, developed to fabricate microstructures with high aspect ratios, have not found extensive industrial application due to their limited flexibility and high operational cost.

Another group of fabrication technologies, such as two-photon polymerization[10,11] and fused deposition modeling,[12,13] are all low throughput methods and are not utilized as mass manufacturing techniques given their serial fabrication nature. Take two-photon polymerization, for example; this method requires the use of two low power pulsed laser beams which intersect deep within a photosensitive liquid resin bath. At the intersection point, the beams form a small volume element that has enough photon flux to polymerize the material. Two beams are then controlled in such a way that the intersection point writes a completely three-dimensional pattern in the resin bath in a serial point-by-point

fashion. This approach comes with several disadvantages. For instance, the choices of resins available for this technique are severely limited due to the need for them to be highly transparent to the laser beams. This transparency requirement also eliminates the possibility of loading the resin bath with ceramic or metal particles thus expanding the available material set. Finally, this technique is limited in its ability to be a rapid manufacturing method due to its inherently serial nature.

Mask lithography has been widely used to produce extruded two-dimensional objects since its development in the 1960s for IC manufacturing. This technique succeeded in the semiconductor industry because of its much higher throughput compared to serial processes. Mask lithography, however, struggles with true three-dimensional components because of expensive masks, the time-consuming process of mask alignment, and difficulties creating high aspect ratio features. In addition, conventional mask-based lithography cannot create curved surfaces in the third dimension.

Projection micro-stereolithography (PμSL) combines high throughput capability of mask lithography with the design flexibility offered by serial processes. PμSL is most similar to mask-based lithography in that the parts are produced in a layer-by-layer process.[14] However, PμSL allows for elimination of many time intensive steps in mask lithography such as mask production and alignment by employing a digital dynamic mask which can dynamically generate and reconfigure patterns of light. Therefore, arbitrary 3D shapes with complex curvatures in all three dimensions can be rapidly fabricated.[15,16]
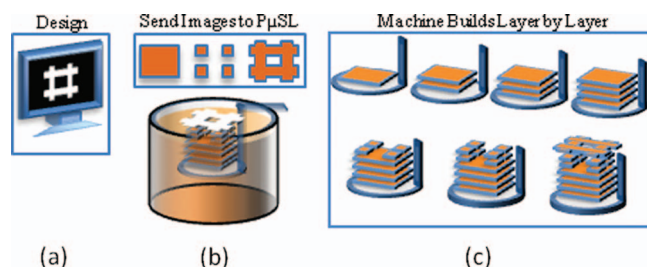
FIG. 1. PµSL operational principle. A three-dimensional model (a) is sliced into layers and sequentially projected onto the photocurable resin (b) and the structure is built in a layer-by-layer fashion (c).

PµSL is a three-dimensional fabrication technology based on a photo-polymerization reaction. To fabricate a three-dimensional object, an image corresponding to each layer is projected onto a monomer resin with ultra-violet (UV) or near UV light. This induces a polymerization reaction that converts the liquid-state monomer resin into a solid layer in the shape of the projected image. The thickness of the resulting layer is determined by the penetration depth of the light, which is controlled by several process parameters including light intensity, exposure time, and the concentration of photo-absorber and photo-initiator. The polymerized layer is then lowered into a resin bath and a new liquid resin layer is formed on top of the polymerized layer. The next image is then transmitted to the dynamic mask in order to polymerize the next layer on top of the preceding one. This process is repeated until the desired number of layers has been fabricated to complete the 3D object. The process is illustrated in Figure 1. Figure 2 describes the optical setup used to produce the projected image. The PµSL additive micromanufacturing technique presented here is highly three-dimensional, can be multi-material, and energy efficient due to its efficient consumption of feedstock material and its use of inexpensive low power components such as near-UV light-emitting diode (LED) arrays instead of lasers. Additionally, microstructures that are fabricated with this technique will provide performance and efficiency benefits to a range of applications.

This paper describes the construction of a high-resolution projection micro-stereolithography system based on a liquid crystal on silicon (LcoS) ch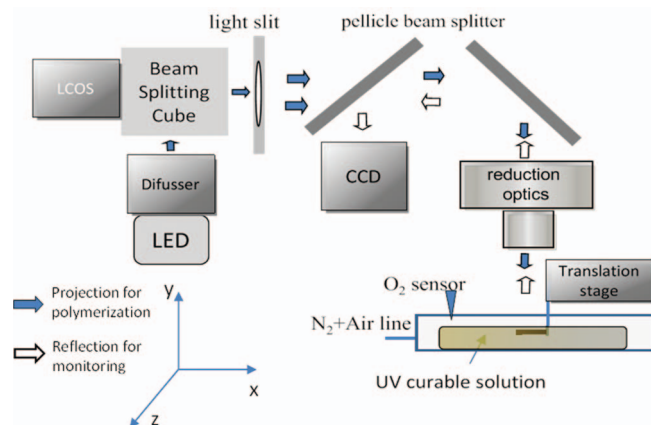ip as the dynamic mask. This work also identifies and investigates process parameters that influence polymerization depth and part quality. We present experimental results that elucidate the effects of various process parameters and demonstrate the ability to reliably fabricate highly complex, high-resolution, three-dimensional, and micro-scale structures for a broad range of applications.

II. MATERIAL AND METHOD

A. Materials and operating principle

PµSL is a process that involves the chemical kinetics of photo-polymerization of UV curable resins consisting of monomer, photo-initiator (PI), and photo-absorber. First, under UV illumination, PI absorb incident photons and generate free radicals. The excited free radicals combine and react with the monomer molecules (M) to form larger reactive molecules. These reactive molecules continue to react with adjacent monomers to form longer polymeric molecules. The polymeric molecules keep growing until two of them combine and terminate the reaction. The solidified polymer structure eventually forms by the entanglement and cross-linking of these polymer chains.

Based on this photo-chemistry, PµSL is capable of rapidly fabricating complex three-dimensional microstructures in a bottom-up, layer-by-layer fashion. A computer-generated 3D computer aided design model is first sliced into a series of closely spaced horizontal planes. These two-dimensional slices are digitized as a bitmap image and transmitted to the LCoS chip which projects the image through a reduction lens into a bath of photosensitive polymer resin (Figures 2 and 4(a)). Once the material in the exposed area is polymerized by the chemical reaction described above, the substrate on which the polymerized material rests is lowered to repeat the process with the next image slice.

Digital masking is the core technology that transforms a slow serial stereolithography process into an extremely rapid and effective parallel process. There are three types of digital mask technologies: (1) liquid crystal display (LCD); (2) digital micromirror device (DMD); and (3) LCoS. LCD is the cheapest and earliest dynamic mask employed in stereolithography. The limitation of LCD as a dynamic mask for photocurable resins comes from the fact that LCD light absorption is significantly higher during the ON mode and, therefore, its use is limited to a small range of commercially available UV curable resins.[17] The DMD offers improved contrast over the LCD and is better suited to handle UV light than LCD. However, DMD tends to mechanically fail when taken out of their sealed environment and is not well suited to a laboratory setup outside of a clean room. In this study, the LCoS chip was employed as the spatial light modulator due to its highly reflective surface coated with liquid crystals which provides high contrast ratio as well as high packing density, small pixel size, and adequate switching speed. In the PµSL system, the LCoS chip works both as a mask and as a shutter. Not only are the sliced bitmap images displayed on it to modulate the illumination light but it also controls the polymerization time by providing the ability to switch completely off creating a non-reflective surface resulting in no light transmission to the resin bath.

FIG. 2. Schematic illustration of the projection microstereolighography system.

A LED was chosen as the light source in the PµSL system. Among many others, the major advantage of LEDs over conventional light sources such as mercury arc lamps and lasers is their energy efficiency. LEDs consume much lower energy than lasers and mercury lamps for polymerization of the same volume of material. Moreover, they are tailored to a specific wavelength to match that of the UV curable resins. Other advantages include shorter starting time, longer lifespan, low cost, compact size, and low heat dissipation. Although the light output of an individual LED is modest, advanced arrays of high power LEDs delivers sufficient light power required for this study.

B. PµSL system operation

Figure 2 depicts the optical configuration of the PµSL system. The LED light source is a 395 nm LumiBright Light Engine (Innovations in Optics, Inc.). Two 20° engineered diffusers (ThorLabs) are used to condition the light. The light intensity measured at the liquid monomer surface can range from 1 mW/cm^2 to 100 mW/cm^2. The system is enclosed in a custom made fabrication chamber with a mass flow sensor in order to monitor the oxygen concentration in the chamber; a critical parameter for repeatable fabrication.

The optical train consists of a beam splitting cube (Tower Optical Corporation: Part 13397) and a 92/8 pellicle beam splitter (ThorLabs). The cube polarizes the light and contains an anti-reflective coating. The pellicle directs light to a CCD camera used to check system focus and to monitor the build.

A LCoS display (Holoeye, Co., model HED-6001) is used as a digital mask in the PµSL system. This display has a resolution of 1920 × 1080 pixels over a 15.36 mm by 8.64 mm area. The manufacturer reports a contrast ratio of 2500:1 and 95% reflectivity. An OEM HDTV kit (Aurora Systems, Inc.) is connected to the LCoS chip to control the display. UV reduction optics (Coastal Optical Systems: Parts 0745200, 0508100, and 0452200) reduces the display pixels by a factor of 6:1, making the final image resolution 1.3 µm/pixel at the projection focal plane.

Light uniformity was further improved using the grayscale capability of the LcoS spatial light modulator. In order to realize improved uniformity, a background correct procedure was developed. A custom LabVIEW program sets all pixels on the LCoS to maximum intensity and captured the resulting image. This image was then processed through a MATLAB script within the LabVIEW program that analyzed the intensity and suppressed the pixel value at regions where the intensity was above the average. This corrected mask was then projected and a new image was taken. This loop was repeated until the intensity variation over all pixels in the projection plane was within the desired range. As shown in Figure 3, this background correction reduced the intensity non-uniformity from 16% to 5% measured from maximum to minimum intensity.

The objects were fabricated using 1, 6-hexanediol diacrylate (HDDA; CAS 13048-33-4) as the liquid monomer which was mixed with 1-phenylazo-2-naphthol (Sudan 1; CAS 842-07-9), a photo-absorber that varied in concentration from 0% to 2% by weight in HDDA to adjust the light penetration
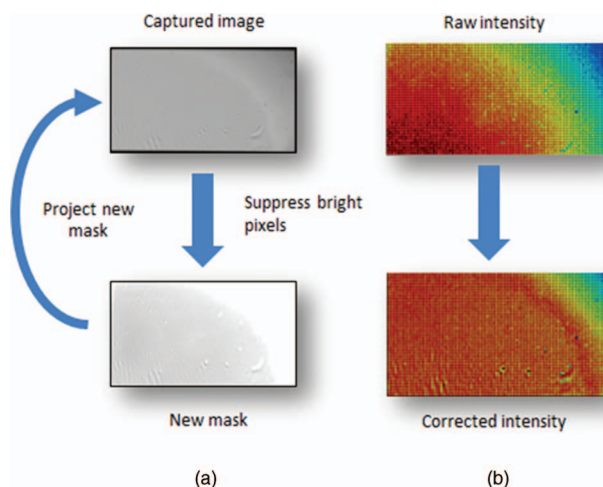

FIG. 3. Image correction procedure for improving light uniformity. (a) Captured blank image and image for background subtraction. (b) Example of normalized intensity heat map before and after correction.

depth, and phenylbis (2, 4, 6-trimethylbenzoyl) phosphine oxide (Irgacure 819; CAS 162881-26-7), a photo-initiator fixed at a concentration of 2% by weight in HDDA.

The substrate travels in the z-direction between each build layer, perpendicular to the fluid surface of the resin bath, and is controlled by a motorized linear translation stage (Newport, Co., UTS150CC). This stage has a resolution of 0.1 µm and a minimum step size of 0.3 µm. The maximum build height is on the order of several centimeters, although no parts were manufactured over 1.5 mm for a single structure. The focusing procedure is summarized in Figure 4(b). A Newport control panel was used to control the position of both the resin bath and the substrate holder. The reflected image from the liquid monomer surface is captured by the camera through the pellicle beam splitter and each projected image
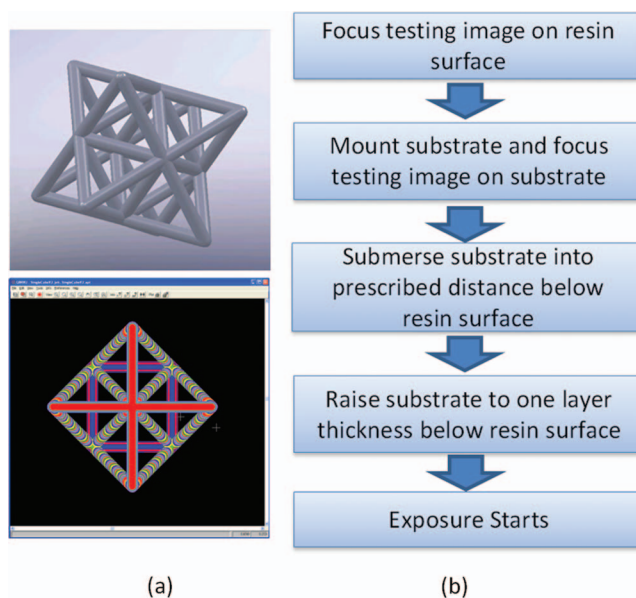

FIG. 4. System operation for fabricating 3D structures. (a) Example of 3D geometric model and the slicing program output used to generate 2D bitmap images. (b) PµSL system operation procedure for focusing and subsequent fabrication.

on the liquid monomer can be monitored in real time from the external monitor connected to the main control computer. The surface of the liquid monomer surface is adjusted so that the projected image from the surface is in focus. To initiate a build sequence, the substrate is moved to the focal point of a projected image. The silicon substrate is then lowered into the monomer and raised to 10 μm below the surface (Figure 2). The first mask is then projected onto the monomer. Between subsequent masks, the substrate is submerged and raised to 10 μm below its previous position.

A custom LabVIEW Virtual Instrument (VI) controlled the system. The user inputs test conditions by means of a text document which specifies exposure time, light power, and z-axis motion distance (hence, layer thickness) between each exposure step. The system then waits a pre-specified time for the disturbed free surface of the liquid material to settle, followed by light exposure for the time and exposure energy described by the text file.

C. PμSL process model

To better understand the polymerization process, we developed a numerical model similar to the one described in Ref. 18. A series of coupled reaction-diffusion equations described the three stages of the curing process: photo-initiation, propagation, and termination, whereas the light attenuation was modeled after the Beer-Lambert law. The independent variables included monomer, photo-initiator, and radical-terminated chain concentrations, light intensity, and temperature. The propagation and termination rate constants as a function of the amount of cross-linking were measured with differential scanning calorimetry.[19] The system of equations was solved on a tetrahedral mesh representing the resin bath with the COMSOL multiphysics software package.

III. RESULTS AND DISCUSSION

A. Photon flux and time study

Experiments were conducted to study the effect of polymerization depth against exposure time and light intensity projected onto the liquid surface. In order to fabricate three-dimensional structures with controlled part thickness and geometries, the polymerization depth under different conditions needs to be measured. This provides the user with an understanding of what conditions must be used to produce free-standing layers of different thicknesses. A time study and a power study were conducted. We compared this information to our simplified model to test its predictive ability.

An array of overhanging bridge structures was fabricated with array of exposure dosage through varying light intensity and exposure time (Figure 5, inset). Each bridge layer represented one polymerization layer and the mean thickness of a given layer was taken to be the polymerization depth. Figure 5 shows the variation of polymerization depth as a function of total exposure dosage E (mW s/cm^2) received from the monomer. This was done by varying the polymerization time and light intensity. The results indicate that the polymerization depth is linearly proportional to the natural
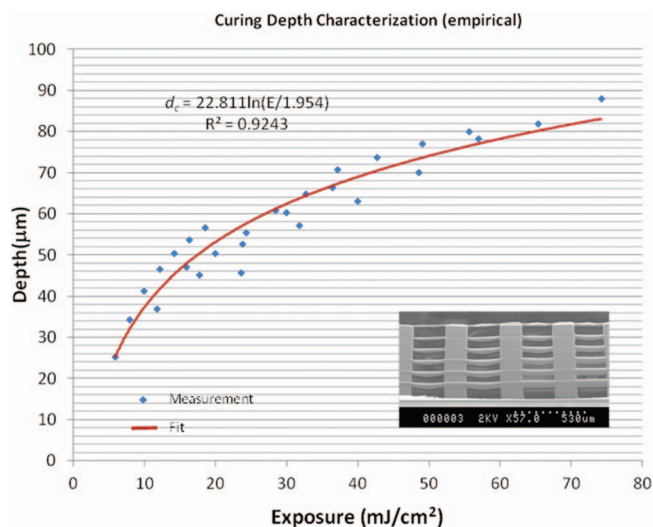

FIG. 5. Photon flux versus polymerization depth. The curing depth increases linearly with natural logarithm of exposure energy. The inset is the suspended multiple-bridge structure for curing depth measurement with multiple flux-exposure time combinations. The experimental condition was 0.4% oxygen, 0.8 Sudan1, and 2% photoinitiator.

logarithm of UV exposure energy, which is in good agreement with the numerical model.

B. Photo-absorber

Sudan 1 is a photo-absorber that limits the exposure depth and spread of polymerization and increases the threshold light flux required. This decreases the sensitivity and makes it more difficult for stray light to polymerize the solution, effectively increasing the contrast of the system. This increases the effective contrast ratio and reduces the minimum layer thickness, which brings the system closer to its maximum theoretical resolution.

To control polymerization depth, the light absorber, Sudan 1 (1-phenylazonaphth-2-ol) was mixed with the liquid pre-polymer and the curing characteristics of the solutions were examined. Sudan 1 also has the effect of reducing the reaction rate by limiting the number of available photons. Based on these results, several complex 3D microstructures with overhanging features were fabricated to illustrate the effects of light absorber concentration on part fabrication. The sensitivity of polymerization depth to photo-absorber concentration is illustrated in Figure 6. For a constant light flux and exposure time, the cure depth decreases with an increase in UV absorber. A saturation point was reached when the concentration of photo-absorber is close to 2% by weight.

C. Parameter sensitivity

An analysis of the sensitivity plot shown in Figure 6 provides information regarding which parameters are most important in controlling polymerization depth. We fabricated a matrix of overhanging bridge structures with an array of normalized parameters, i.e., exposure flux, exposure time, and photo-absorber concentration (Sudan 1) against polymerization depth measured with a scanning electron microscope
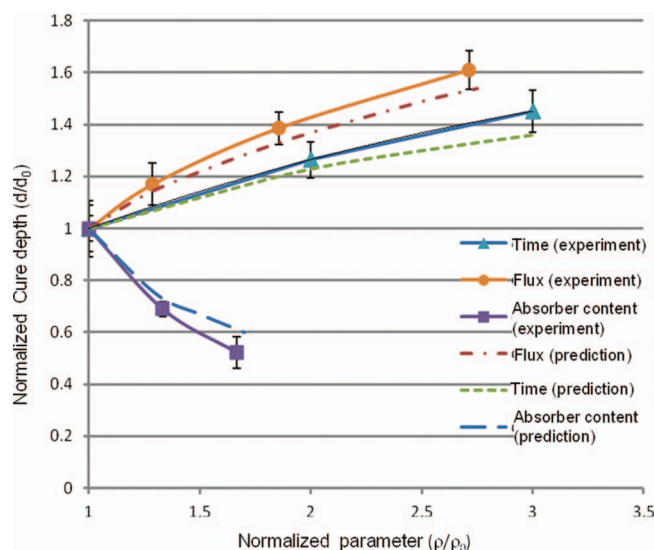
FIG. 6. Fabrication parameter sensitivity on curing depth. The dotted lines are numerical predictions. The solid lines are experimentally measured polymerization depths against normalized system parameters.

FIG. 7. Variations of polymerization depth with change in ambient oxygen concentration. The exposure power was set as 0.809 mw/cm^2 for a time duration of 30 s, Sundan1 concentration was 0.8%.

(Hitachi *S800 SEM*). Figure 6 shows the effect of four sets of control parameters on the polymerization depth measured from suspended multi-bridge structures shown in the inset of Figure 5. The effect of photo-absorber, light flux, and exposure duration are all numerically and experimentally studied.

The plot indicates that light intensity and photo-absorber concentration had the greatest effect on exposure depth. An increase in light intensity will produce a deeper polymerization for a given exposure time. For a constant light flux and exposure time, the polymerization depth will decrease with an increase in photo-absorber. With a constant photo-absorber concentration, the polymerization depth marginally increased with an increase in photo-initiator. This suggests that limited gains will be achieved by using more than the 2% photo-initiator concentration in this study.

D. Oxygen inhibition

In addition to the propagation and termination reactions, oxygen in the reaction volume acts as a radical scavenger and inhibits the propagation and termination steps of the reaction mechanism. Loss of radicals to oxygen is a problem that is pervasive in free radical polymerization reactions. Oxygen competes strongly for the radicals to form a stable peroxy radical. Until most of the oxygen in the reaction volume has been used via reaction with radicals, there is very little consumption of the monomer. The concentration of oxygen in the ambient atmosphere was monitored using an oxygen sensor from Ocean Optics and controlled by tuning and stabilizing a N$_2$ flow into the fabrication chamber. Figure 7 illustrates the effect of oxygen on polymerization depth. As the concentration of oxygen increases, the oxygen serves as the threshold on photo-polymerization as it competes for radicals with monomer consumption. Thus, the effective control of oxygen concentration is critical to controlled and repeatable fabrication.
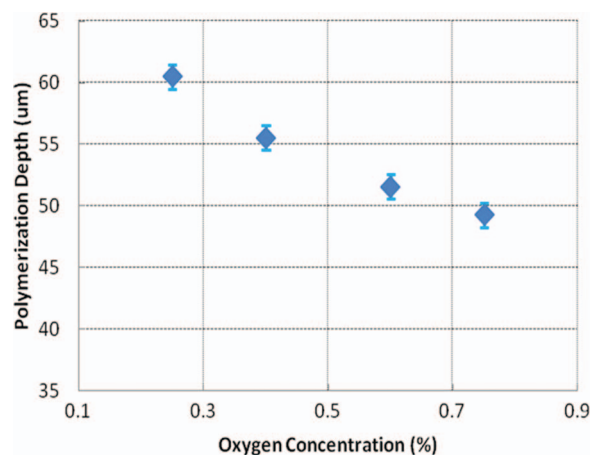
E. Fabrication of three-dimensional structures with complex architectures

The PμSL system is capable of manufacturing a variety of three-dimensional structures with precise control of geometry. Figures 8(a)–8(d) illustrate the ability to fabricate arbitrary three-dimensional overhanging structures with defined complex curvature, multiple suspending structures, and cellular structures such as micro-lattice architectures and porous materials which were not achievable by previous 3D fabrication techniques. No current technology is able to rapidly
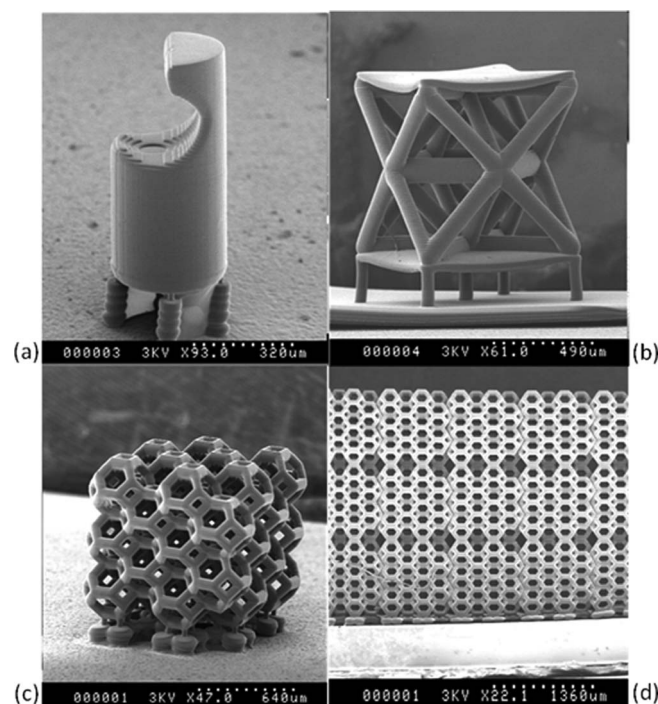

FIG. 8. Complex three-dimensional structures manufactured with the PμSL system. (a) Micro-gripper structure with overhanging gripper and pre-defined curvature. (b) Micro-lattice unit cell structure. (c) Porous structure with tetrakaidehedron unit cell architecture. (d) 5 × 3 × 3 mm^3 porous structure assembled from multiple porous unit cells from (c) using the step-and-repeat process.
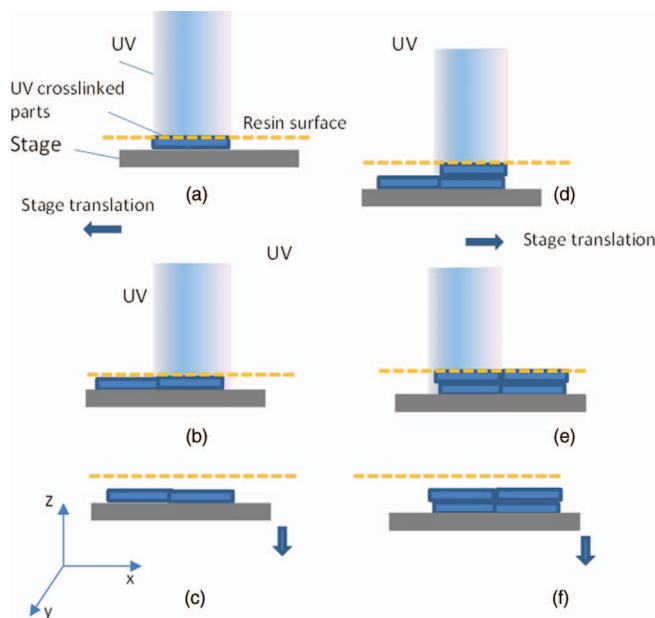
FIG. 9. Schematic illustration of the step-and-repeat process. (a) Exposure of sub-area. (b) Exposure of the next sub-area after stage lateral movement. (c) Stage moves down and new layer of pre-polymer resin flows over and settles on top. (d) Exposure of new sub-area. (e) Exposure of the next sub-area. (f) Stage moves down and process repeats.

and sustainably produce such structures with optimized three-dimensional architectures at the meso- and micro-scales while also being flexible enough to vary the geometry from part-to-part.

In addition, the fabrication system can be expanded to manufacture meso-scale structures (ranging from mm to cm in length) with micro-scale architectures. This will expand far beyond the fabrication area of the previous (up to 1 mm × 1 mm) 3D fabrication techniques. This was achieved by a step-and-repeat process. The total fabrication area was divided by the maximum projection area into multiple sub-areas. When fabricating one layer with multiple subareas, after exposure of one sub-area, the LED light turns off and the translation stage moves horizontally to the next sub-area and the exposure process continues. This process is repeated until all sub-areas have been exposed. After the completion of one layer, the translation stage steps down and the same process is repeated. Figure 9 illustrates this process and a large scale structure with micro-scale tetrakaidecahedron[20,21] is demonstrated in Figure 8(d).

IV. CONCLUSIONS

This paper discusses the design and optimization of a projection micro-sterelithography system for fabricating highly complex three-dimensional micro-scale structures unachievable by other fabrication technologies. The core of the system was based on an LCoS chip used as a dynamic digital mask with a UV LED light source. Images were projected onto a UV curable resin bath enclosed in an environmental chamber with precisely controlled ambient oxygen concen-

tration. To investigate the effects of various process control variables, an experimental parametric study was performed to determine those that were most important. The effect of oxygen content on polymerization depth was found to have inhibiting but minimal effect on part quality as compared to other control parameters. The sensitivity predicted by a process model was comparable to the depth variation observed in the manufactured parts. The optical intensity and photo-absorber concentration are identified as the most influential factors. Finally, we demonstrated the utility of the optimized system by producing a variety of micro-structures with complex geometries and explored the potential of using the system to build meso-scale structures with micro-scale architecture. These achievements pave the way for large scale micro- and nano- manufacturing that extends the current state of art of three-dimensional fabrication technologies.

[1]K. Arcaute, B. K. Mann, and R. B. Wicker, Tissue Eng. **17**(1), 27–38 (2011).
[2]Y. Miyamoto, S. Kirihara, M. W. Takeda, K. Honda, and K. Sakoda, Mater. Sci. Forum **492–493**, 77–83 (2005).
[3]J. Sanjuan, A. Lobo, M. Nofrarias, J. Ramos-Castro, and P. J. Riu, Rev. Sci. Instrum. **78**(10), 104904–104913 (2007).
[4]A. N. Das, R. Murthy, D. O. Popa, and H. E. Stephanou, IEEE Trans. Autom. Sci. Eng. **9**(1), 160–170 (2012).
[5]X. Y. Zheng and X. Zhang, J. Micromech. Microeng. **18**(12), 125006 (2008).
[6]J. Hersener, E. Piper, A. Wilhelm, and G. Birkenstock, J. Vac. Sci. Technol. B **5**(1), 253–256 (1987).
[7]H. van Santen and J. H. A. Neijzen, Opt. Microlithography Xvi, **5040** (Pts 1-3), 1750–1755 (2003).
[8]S. J. Moon, S. S. Lee, H. S. Lee, and T. H. Kwon, Microsyst. Technol. **11**(4-5), 311–318 (2005).
[9]Y. N. Xia and G. M. Whitesides, Annu. Rev. Mater. Sci. **28**, 153–184 (1998).
[10]Z. P. Liu, Y. Li, Y. F. Xiao, B. B. Li, X. F. Jiang, Y. Qin, X. B. Feng, H. Yang, and Q. H. Gong, Appl. Phys. Lett. **97**(21), 211105 (2010).
[11]K. Venkatakrishnan, S. Jariwala, and B. Tan, Opt. Express **17**(4), 2756–2762 (2009).
[12]M. Centola, A. Rainer, C. Spadaccio, S. De Porcellinis, J. A. Genovese, and M. Trombetta, Biofabrication **2**(1), 014102 (2010).
[13]C. S. Wang, T. R. Chang, W. H. A. Wang, and M. C. Lin, Adv. Mater. Process. **443**, 522–527 (2010).
[14]C. Sun, N. Fang, D. M. Wu, and X. Zhang, Sens. Actuators, A **121**(1), 113–120 (2005).
[15]H. Lee, C. G. Xia, and N. X. Fang, Soft Matter **6**(18), 4342–4345 (2010).
[16]H. Lee, J. P. Zhang, H. Q. Jiang, and N. X. Fang, Phys. Rev. Lett. **108**(21), 214304–214308 (2012).
[17]H. Xu, A. B. Davey, T. D. Wilkinson, W. A. Crossland, J. Chapman, W. L. Duffy, and S. M. Kelly, Mol. Cryst. Liq. Cryst. **411**, 1121–1133 (2004).
[18]N. Fang, S. Sun, and X. Zhang, Appl. Phys. A **79**(8), 1839–1842 (2004).
[19]G. R. Tryson and A. R. Shultz, J. Polym. Sci. Pol. Phys. **17**(12), 2059–2075 (1979).
[20]D. T. Chalkley, Science **118**(3072), 599–600 (1953).
[21]L. J. Gibson, MRS Bull. **28**(4), 270–271 (2003).